# An fMRI examination of the neural processing of periodic motion trajectories

**Diana J. Gorbet** Centre for Vision Research, York University, Toronto, ON, Canada

**Frances Wilkinson** Centre for Vision Research, York University, Toronto, ON, Canada

**Hugh R. Wilson** Centre for Vision Research, York University, Toronto, ON, Canada

Perception of periodic or closed-circuit motion trajectories plays a crucial role in our ability to learn and perform many common skilled actions. For example, periodic trajectories are a key component of many types of biological movements when viewed relative to body translation. In the current fMRI study, we used a novel visual stimulus consisting of a target moving along a closed trajectory defined by a radial frequency (RF) pattern (i.e., a sinusoidal variation of trajectory radius relative to a circular trajectory) to determine which brain regions encode these periodic movement paths. Multivoxel pattern analyses permitted prediction of the shapes of different periodic trajectories within regions V2 and V3 indicating that these regions play a role in the processing of periodic visual motion. In addition, blood oxygen level dependent (BOLD) responses associated with the presentation of targets moving along RF trajectories compared with nonperiodic motion and static RF shapes revealed significantly greater activity in visual areas V1, V2, V3, V3A, and V4. To our knowledge, the results of this study represent the first examination of the functional brain activity underlying periodic motion processing and should inform further study.

Keywords: visual motion perception, periodic motion, radial frequency, fMRI

Citation: Gorbet, D. J., Wilkinson, F., & Wilson, H. R. (2012) An fMRI examination of the neural processing of periodic motion trajectories. *Journal of Vision*, *12*(11):5, 1–15, http://www.journalofvision.org/12/11/5, doi:10.1167/12.11.5.

## Introduction

Periodic closed-circuit motion refers to a cyclical movement trajectory where each cycle of motion begins and ends in the same location, forming a closed circuit. At present the perception of this unique class of visual motion remains almost entirely unexplored. One exception is a study by Todd (1982) in which stimuli consisted of line segments with endpoints moving in periodic trajectories. Observers in this study were able to reliably detect the difference between rigid and nonrigid motion paths based on deformations of otherwise elliptical trajectories. In addition, a recent study by Or, Thabet, Wilkinson, and Wilson (2011) demonstrated that deviations from a circular movement path as small as 1 min of arc can be detected by observers viewing a dot moving in periodic trajectories that subtend 1° of visual angle. The authors also showed that observers could reliably identify the shape of the trajectories. Thus, it has been demonstrated that human observers are very sensitive to closed-circuit visual motion. However, to our knowledge no study to date has looked at the functional neural activity underlying periodic motion perception.

Although little is known about how the brain processes periodic visual motion, this type of movement trajectory forms an important component of many types of biological motion viewed relative to body translation. For example, during rhythmic movements like walking or riding a bicycle, the motion paths of joints, such as the knee, and parts of the body, such as the feet, form a periodic trajectory that begins and ends in the same location (with respect to the rest of the body) for each cycle of the body's movement (Johansson, 1973; Johansson, 1976; Tsai, Shah, Keiter, & Kasparis, 1994). In addition, cyclic movements are also often observed in gestural hand motions that convey important nonverbal information during communication (Ladewig, 2011; Xiong & Quek, 2006). Therefore, closed-circuit visual motion forms an integral component of many human movements suggesting that the perception of periodic motion may play a role in our ability to learn,

doi: 10.1167/12.11.5 Received February 14, 2012; published October 9, 2012 ISSN 1534-7362 

perform, and understand many common skilled actions.

Humans are extremely good at recognizing movements made by other people and can form accurate impressions of the nature of biological motion based solely on the presentation of a few points of light describing the motion of the main joints of an actor performing a movement (Johansson, 1973). In fact, people are so good at perceiving what actions these *point light* presentations are portraying that they can often tell not only what action is being performed, but also information such as the actor's mood and gender (Barclay, Cutting, & Kozlowski, 1978; Dittrich, Troscianko, Lea, & Morgan, 1996; Mather & Murdoch, 1994; Troje, 2002). Importantly, it is clear that the percept of a moving human from point light animations is conveyed not just from global processing of the entire set of moving points, but also from the movements of individual dot locations (Chang & Troje, 2009; Hirai, Saunders, & Troje, 2011; Troje & Westhoff, 2006). For example, observers can tell which direction a point light animation is facing even when viewing a fully scrambled display (Troje & Westhoff, 2006). However, the possible contribution to this processing of periodic motion trajectories at individual body locations has not yet been assessed.

In this study, we used fMRI to ask which regions of the brain respond to periodic movement paths and further, whether the spatial pattern of activity within selected visual regions of the brain is predictive of specific trajectory shapes. In this study, we presented participants with a dot moving along radial frequency (RF) motion trajectories that were based on deformations of a circular motion path (Or et al., 2011). Specifically, RF patterns are comprised of sinusoidal modulations of the radius of the trajectory in polar coordinates (Wilkinson, Wilson, & Haback, 1998). Humans are extremely adept at detecting very small deviations from a circular form in static and motion patterns (Or et al., 2011; Rainville & Wilson, 2004; Wilkinson et al., 1998) and can consistently identify the shapes of RF motion trajectories (Or et al., 2011). These characteristics make RF motion stimuli an excellent tool for beginning to investigate the neural correlates of the perception of periodic motion.

In the results presented below, we demonstrate that blood oxygen level dependent (BOLD) fMRI activity evoked by RF motion trajectories is significantly greater than that evoked by either static RF shapes or open trajectory visual motion in several visual regions. Further, the spatial pattern of voxel activity in visual areas V2 and V3 varies in a predictable manner depending on the characteristics of the shape of the periodic motion that is being observed, indicating that these regions may have a role in encoding the shapes of these trajectories.

# Methods

## Participants

Participants in the study included six men and four women (mean age 32.9 ± 1.6 years). All participants had normal or corrected-to-normal vision and were right-handed. The York University Research Ethics Board human participants subcommittee approved the protocol used for the experiment. The experimental protocol was in compliance with the Declaration of Helsinki. All participants provided written informed consent prior to data collection.

## Stimulus

We used a novel visual stimulus consisting of a dot moving along a periodic trajectory defined by a radial frequency (RF) pattern. RF motion trajectories were produced by applying a sinusoidal temporal modulation to the radius of an otherwise circular trajectory centered about a fixation cross such that the dot moved at angular speed $v$ and the dot's polar location $r$ at time $t$ was defined as

$$r(vt) = r_0\Big(1 + \mathrm{A}\sin(\omega \mathrm{vt} + \phi)\Big), \quad (1)$$

where $r_0$ is the mean radius, A is the radial modulation amplitude, ω is the radial frequency, and φ is the phase angle of the trajectory (Or et al., 2011). The movement of the dot traced a trajectory that always began from a point directly to the right of the fixation cross, moved in a clockwise direction around the cross, and then ended at the location from which it began (Figure 1). Importantly, during the presentation of these stimuli, participants only saw the moving dot (i.e., the shape of the RF trajectory itself was never displayed). The mean radius ($r_0$) was set to 2° of visual angle. Radial frequencies (ω) from two to five cycles were tested during the experiment.

Both amplitude (A) and phase angle (φ) were varied from trial to trial to prevent adaptation to the stimuli. Phase angle defines the orientation of the trajectory. Changing this value results in a rotation of the shape described by the trajectory of the moving dot but does not alter the starting position of the dot on the screen. Amplitude defines the size of the sinusoidal deviation of the radius relative to a circular trajectory. Or et al. (2011) demonstrated that RF trajectories ranging from two to five cycles can be identified with greater than 72% accuracy with radial deformations of seven times detection threshold. Therefore, in the study presented here, to ensure that observers were able to easily identify RF motion trajectories, the amplitude of radial

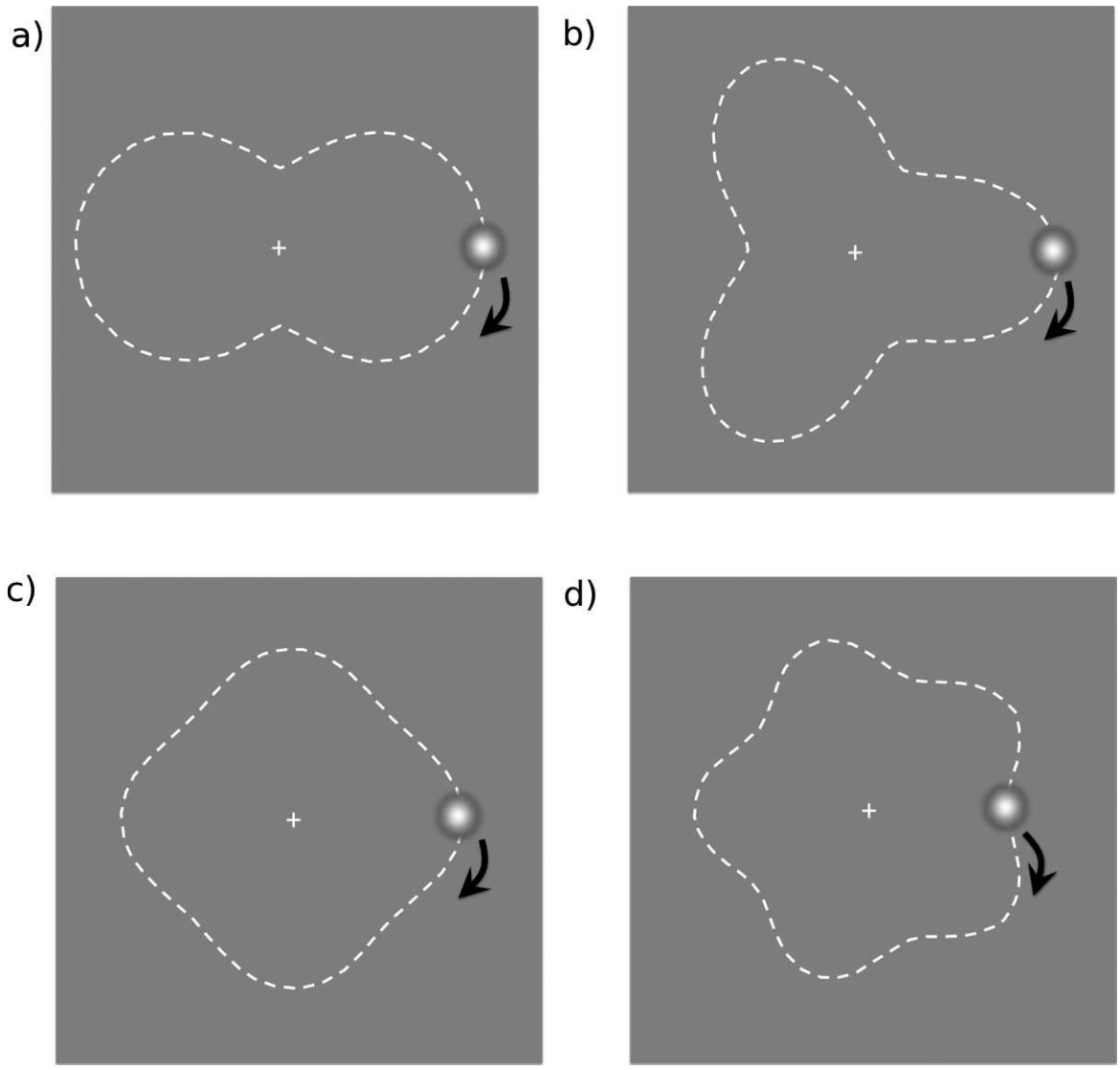


Figure 1. Schematic representation of example periodic radial frequency (RF) motion trajectories. The movement of the dot traced a trajectory that always began from a point directly to the right of the fixation cross, moved in a clockwise direction around the cross, and then ended at the location from which it began. Observers only saw the dot and fixation cross (i.e., the shape of the trajectory was not visible). Samples of trajectory shapes: (a) RF2 trajectory, (b) RF3 trajectory, (c) RF4 trajectory, and (d) RF5 trajectory.

modulations ranged from 20 to 30 times higher than mean detection thresholds. The moving dot itself consisted of a radially symmetric difference of Gaussians (DOG) defined as follows:

$$\mathrm{DOG}(R) - 1.8\ \exp(-R^2/\sigma^2) - 0.8\ \exp\left(-R^2/(1.5\sigma)^2\right), \quad (2)$$

where $R$ is the radius of the DOG and σ was set to 7.1 min of arc such that the peak spatial frequency was 2.74 c/deg and the bandwidth was 1.79 octaves at half-amplitude. The dot was presented with a contrast of 100% and subtended a visual angle of approximately 0.6°.

The stimuli were projected onto a screen that was viewed by subjects via a mirror measuring 16 × 12 cm placed over the headcoil. The approximate distance of subjects' eyes to the mirror was 13 cm (depending on individual head size and position within the headcoil). The resolution of the projector was 1280 × 1024 and the refresh rate was 60 Hz.

## MRI data acquisition

Data were collected using a 3T Siemens Magnetom Avanto MR system with a 32-channel head coil, located at York University. Functional images were obtained using T2*-weighted, gradient echoplanar

imaging, FOV = 192 mm, TR = 1.25 s, TE = 30 ms, and flip angle = 90°. Twenty 4-mm thick slices were acquired (acquisition of data from slices was interleaved) with a voxel dimension of 2 × 2 × 4 mm and zero gap. For each participant, slices were placed to ensure complete coverage of the entire occipital and temporal cortices. T1-weighted anatomical images were collected using 192 slices in the sagittal orientation, TR = 1900s, TE = 2.44 s, flip angle = 9°, FOV = 240 mm, and a voxel dimension of 0.93 × 0.93 × 1.0 mm.

## MRI data collection and analysis

A day or two prior to MRI data collection, each participant took part in a 30 min training session during which time they were shown and then practiced the experimental tasks. All participants received the same amount of training and demonstrated an understanding of the task requirements and a good ability to discriminate between RF motion trajectories prior to entering the scanner.

MRI data acquisition was divided between two sessions (described in greater detail in the following sections). In the first session, participants performed functional runs designed to localize regions of interest (early visual regions, region MT, and regions involved in processing biological motion). Including setup time, the localizer session took approximately 45 min. In the second session, participants performed functional runs designed to test the hypotheses of the experiment. This experimental session took approximately one and a half hours. High-resolution T1-weighted scans were also obtained during each of the two sessions to allow for more accurate coregistration of functional images from each session with their associated anatomical scans.

## Localizer scans

### *Retinotopic mapping of early visual areas*

Retinotopic mapping was performed to delineate the borders between early visual areas V1, V2, V3, V3A, and V4 (Engel, Glover, & Wandell, 1997; Sereno et al., 1995). Rotating contrast-reversing (8 Hz) checkerboard wedges had a polar angle of 45° and spanned a visual angle of approximately 0.4° to 6° eccentricity. A small central fixation dot randomly changed color every 0.5 to 3.0 s. To ensure that participants maintained central fixation, they were required to press a button each time the fixation dot changed to the color red. Each full cycle of rotation lasted 40 s (i.e., for each cycle, the wedge moved around the central fixation dot to eight locations and remained at each location for a total of 5 s). The run consisted of an initial fixation lasting 6.25 s followed by eight cycles of the rotating wedge and final fixation period of 12.5 s to allow the hemodynamic response to return to baseline. Therefore the total duration of the run was approximately 5 min 39 s.

Cross-correlation analyses of BOLD signal phase-lag in response to stimulation were used to generate retinotopic maps (for example, see Slotnick & Yantis, 2003). In particular, each cycle of the time-series was segmented into eight phases (corresponding to the eight locations of the wedge) and for each phase a hemodynamic response model was cross-correlated with the time series of each voxel. Voxels surpassing a correlation of 0.20 were then assigned a color associated with the stimulus phase that resulted in maximal correlation. This process resulted in a map that was projected onto an inflated and flattened cortical surface representation obtained for each participant from high resolution T1-weighted anatomical MRIs. The borders between early visual areas were identified as reversals in the phase of map coloration and regions of interest were defined for each participant using these borders (Figure 2).

### *MT localizer*

Visual region MT was localized using a single functional run that was approximately 5 min in duration (Tootell et al., 1995; Watson et al., 1993; Zeki et al., 1991). Observers viewed alternating blocks of either coherently translating dots that changed direction at random intervals (ranging from approximately 2 to 5 s) or blocks of static dots. Four blocks of each of the two conditions were presented in a random order. Each block was 16.25 s in duration and separated by a baseline fixation period of equal duration. Observers were instructed to fixate on a central cross for the entire localizer run. MT was localized robustly and bilaterally in all subjects by contrasting the response to moving dots with that evoked by stationary dots (for an example, see Figure 2).

### *Biological motion processing regions localizer*

Superior temporal sulcus regions involved in processing biological motion were isolated using a block design localizer run where blocks contained either intact point-light animations or scrambled animations consisting of 12 white dots on a gray background (Grossman & Blake, 2001; Grossman et al., 2000; Peelen & Wiggett, 2006). In intact animations, dots were placed in the region of the actor's head and limbs and the animations portrayed the entire body performing simple actions such as kicking or jumping. In scrambled animations, the overall density of dot locations was kept to the same region in which intact animations were located on the screen and the motion trajectory of each individual dot was kept intact, but

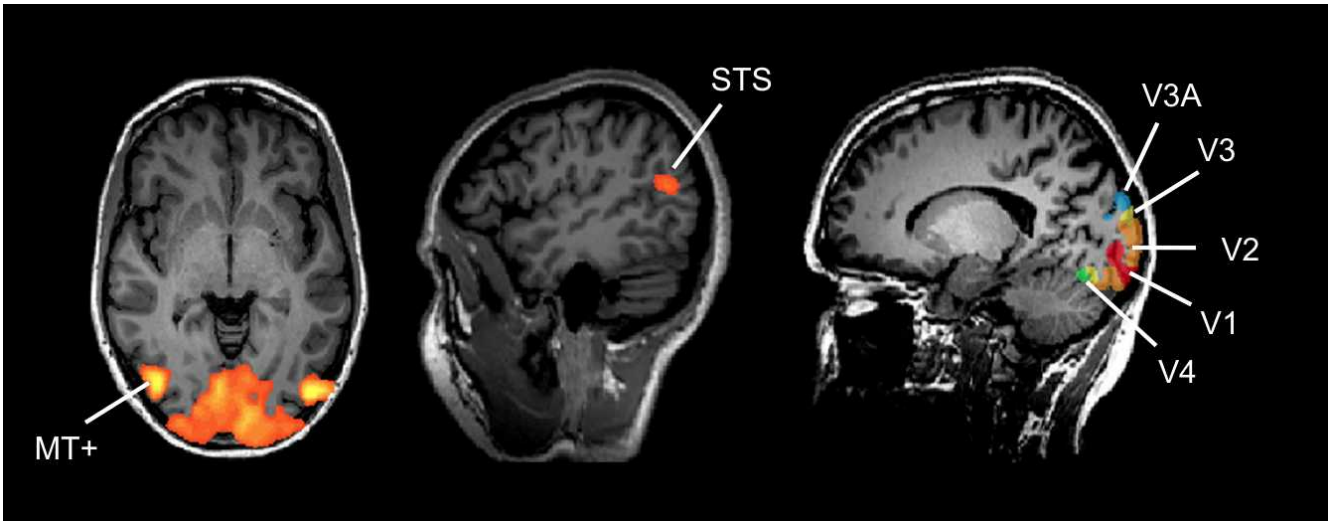


Figure 2. Examples of regions isolated using localizer runs in a single participant.

the spatial location of dot motion starting points was randomized. Each block was 32.5 s long and consisted of 15 animations. The entire localizer run was slightly over 5 min long and contained three blocks of intact animations and three blocks of scrambled animations in random order and separated by fixation periods lasting 16.25 s. Each animation within a block was approximately 1.5 s in duration and animations were separated within each block with short blank fixation intervals.

## Analysis of localizer data for isolation of regions of interest

In addition to the descriptions of data analysis for region of interest localization described in the sections above, it should be noted that all functional localizer data underwent correction for motion using the volume temporally closest to the anatomical scan acquisition as the reference volume. Head movement did not exceed 1 mm in any direction for all participants. In addition slice time correction and linear trend removal were applied to each localizer run and the data were spatially smoothed using a 4 mm full width at half maximum (FWHM) isotropic kernel. Regions of interest were localized both in native subject space (for use with experimental runs designated for multivoxel pattern analysis) and in Talairach space (for use with general linear model analysis of experimental runs).

## Experimental scans

During the experimental session, participants performed two types of block design runs: runs designated for multivoxel pattern analysis (four runs in total) and runs designed to compare RF motion stimuli with both open trajectory motion and static images of RF patterns (three runs in total). Both types of runs were approximately 8.5 min in duration and both types consisted of 25 s blocks separated by 16.25 s fixation-only intervals.

Runs designated for multivoxel pattern analysis (MVPA) contained only radial frequency (RF) motion stimuli. Each block contained a single frequency of trajectories (in other words, two, three, four, or five cycles). Three blocks of each frequency of RF trajectory were performed within each run (making a total of 12 blocks per run) in a pseudorandom order. Within each block, a total of seven separate trajectories were shown and the amplitude and phase of each trajectory was varied to prevent participants from adapting to the stimulus. The time taken for the dot to trace an entire trajectory was 3.3 s and trajectories were separated with 0.33 s interstimulus intervals. Within each of these blocks, one of the seven trajectories formed a perfect circle rather than an RF motion shape. Participants were required to respond to the appearance of a circle by pressing a button, thus ensuring that attention was paid to the task.

Runs designated for comparisons of periodic motion, open trajectory motion, and static radial frequency patterns were structured similarly to MVPA-designated runs. However, in these runs, blocks containing RF motion consisted of either RF2 or RF3 motion paths only; RF4 and RF5 were not presented.

Blocks containing static images of RF patterns consisted of either RF2 or RF3 shapes. Static RF shapes were constructed to be as similar to the RF motion trajectories as possible. Like the motion stimuli,

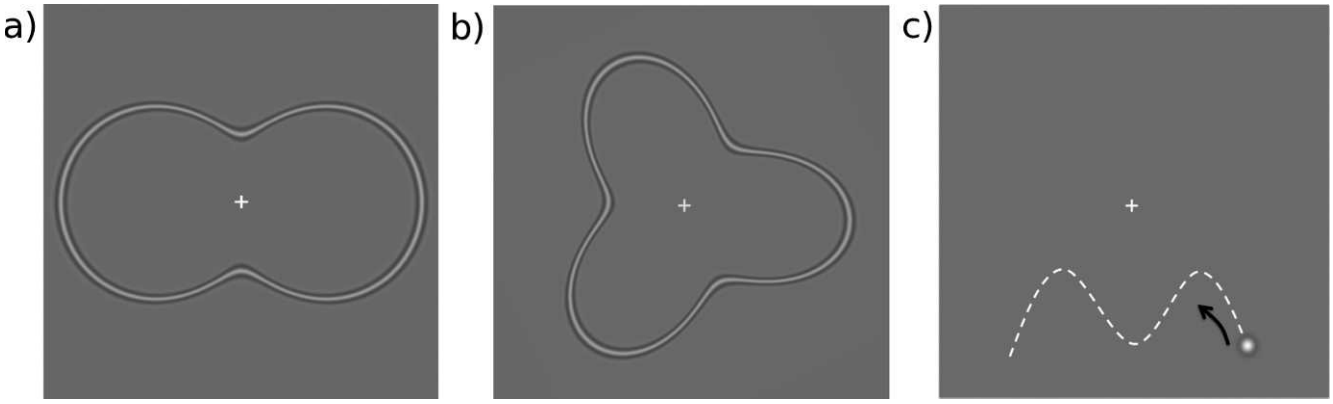


Figure 3. Examples of static RF patterns and open trajectory motion stimuli used in comparisons with RF motion stimuli. (a) RF2 static image, (b) RF3 static image, and (c) open trajectory moving leftward under the fixation cross.

the mean radius of the static RF shapes subtended a visual angle of 2° and identical ranges of radial modulation amplitudes, and phase were used (Figure 3).

Open trajectory motion paths consisted of a DOG dot with the same properties of that used in the RF motion stimuli moving along either two or three cycles of a sine wave. For each open trajectory stimulus, the motion was either rightward above the fixation cross or leftward below the fixation cross to approximately match the overall range of motion covered during presentation of RF motion trajectories which always started to the right of the fixation cross and then moved clockwise around it. Also, to help further equate the open trajectory stimuli with the RF motion stimuli, the dot moved at an eccentricity of 2° of visual angle relative to fixation (Figure 3).

All three types of stimuli (RF motion trajectories, open sinusoidal motion trajectories, and static RF patterns) were presented for 3.3 s each with 0.33 s interstimulus intervals. In order to encourage participants to pay attention to stimulus presentations, one trajectory in RF motion blocks was a perfect circle and required a button press upon detection. Analogously, button presses were required in open trajectory movement blocks upon detection of a straight-line trajectory (rather than a sine wave) and in static image blocks upon detection of a perfectly circular shape. See Figure 4 for a schematic representation of example run time-courses.

## Experimental session data analysis

All analysis of fMRI data was performed using BrainVoyager QX (version 2.2, Brain Innovation, Maastricht, The Netherlands). Functional data from runs designated for MVPA were analyzed separately from those collected to compare activity evoked by RF motion trajectories, open trajectory visual motion, and static images of RF patterns.

## Multivoxel pattern analysis

Preprocessing of functional data from the four MVPA-designated runs from each subject included correction for motion using the volume temporally closest to the anatomical scan acquisition as the reference volume. Traces of head motion in six directions were viewed immediately after data collection on the MRI control room computer for every functional run. Any imaging run in which a participant moved more than 1 mm in any direction was discarded. This criterion resulted in a total of two runs, one from each of two different participants being eliminated; however, viewing head motion profiles in the control room meant that the participants could be asked to repeat the runs within the same data collection session. Therefore, full sets of four useable runs were collected from all participants for multivoxel pattern analysis. In addition, prior to analysis, functional data, head motion graphs, and movies generated by the analysis program were also visually examined to confirm that head movement did not exceed 1 mm in any direction and to look for scanner-related artifacts in the data. Slice time correction and linear trend removal were also applied to each run. Spatial smoothing was not performed and functional data were left in native subject space (rather than Talairach transformed).

A multiclass linear support vector machine classification approach was used to test whether activity associated with specific radial frequency motion trajectory shapes could be discriminated within the spatial fMRI response patterns in regions of interest. Input into the classification analysis consisted of $t$ value response pattern estimates. We chose $t$ values rather than beta estimates in order to help suppress the contribution of any noisy voxels, which can have high

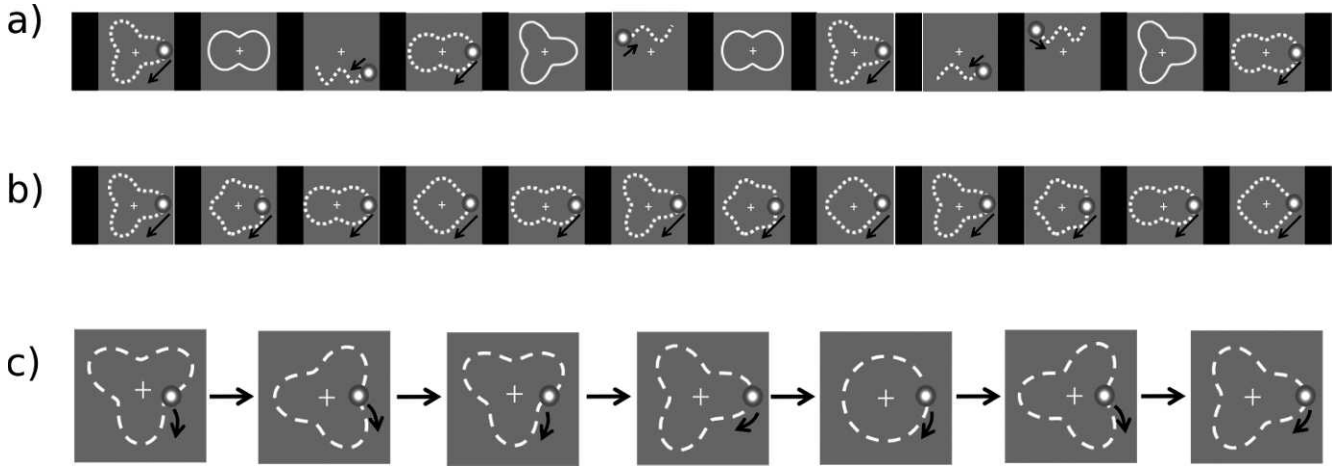


Figure 4. Diagrammatic representations of the experimental paradigm. All experimental data collection runs were approximately 8.5 min long. Each block was 25 s and was both preceded and followed by a 16.25 s fixation only interval. (a) Example of a run used for comparisons of activity evoked by radial frequency (RF) motion trajectories, static images of RF patterns, and open trajectory motion. (b) Example of a run used for multivoxel pattern analysis (MVPA) with blocks of RF2, RF3, RF4, and RF5 motion trajectories. (c) An example of one RF3 motion block. Within each block, the amplitude and phase of each trajectory presentation were varied. To maintain attention, participants were required to respond with a button press when a circular trajectory was detected once per block.

beta estimates as a result of noise alone (Misaki, Kim, Bandettini, & Kriegeskorte, 2010). Standard general linear model (GLM) contrasts of activity associated with each of the four types of RF motion trajectories (i.e., RF2, 3, 4, and 5) did not reveal any significant differences in the mean BOLD signal associated with any of the different trajectory shapes within any of the regions of interest examined. However, as an added precaution for the multivoxel pattern analysis, the signal values for each voxel were *z*-normalized to remove differences in mean activation levels associated with each category (i.e., the four different classes of RF motion trajectories). A *leave-one-run-out* cross-validation permutation test approach (using 1,000 permutations) was used within each region of interest (Nichols & Holmes, 2001). For each subject, data from all but one of the four MVPA-designated runs was used as training data for the creation of the classifier's discriminant function. The left out run (which was completely independent of the data used for both region of interest selection and classifier training) was then used as test data to evaluate the classifier's performance. This process was then repeated until each run had been used for test data once, resulting in a four-fold cross-validation. The mean classifier accuracy (measured as percent correct classification) across the four folds was used as the estimate of the classifier's performance for each participant. Statistical significance was defined as mean classification accuracy of the test data meeting or exceeding the 95th percentile of the distribution obtained via permutation testing, indicating that the classifier performed significantly above chance level.

## General linear model contrasts of activity

A general linear model region of interest analysis approach was used for runs in which multiple types of stimuli were presented (i.e., radial frequency [RF] motion trajectories, open trajectory motion, and static images of RF patterns). Preprocessing of the data included correcting for head movement using the volume closest to the time of anatomical scan acquisition as the reference volume. As with MVPA data described above, head motion parameters were viewed in the MRI control room immediately after collection of each functional run to verify that movement was less than 1 mm so that runs could be repeated if necessary. In total, one participant repeated one run due to head movements in the scanner. Also, during preprocessing, visual inspection of the data and head movement graphs and movies confirmed that all runs included in the final analysis did not contain head movements over 1 mm and that the data was free of scanner-related artifacts. Slice time correction, linear trend removal, and spatial smoothing of 4 mm were also applied to each functional run. Data were also normalized to Talairach space by locating the midpoint of the anterior commissure (AC). The brain was then rotated around this point such that the posterior commissure (PC) appeared in the same axial plane and the line between the AC and PC formed the basis of the *y*-axis of the Talairach coordinate system. The *x*- and *z*- axes were defined, respectively, as running through the AC point from the left to right hemisphere and from the inferior to superior parts of the brain at 90° from the *y*-axis. The brain was then further rotated around the AC–PC axis until the *y*–*z* plane best

separated the two hemispheres. A bounding box consisting of a cuboid enclosing the edge of the cortex was defined as running parallel to the three axes. This main cuboid was separated into subcuboid spaces with an axial plane defining regions above and below the AC–PC line, a plane separating the left and right hemispheres, and planes added to define regions anterior to the AC, between the AC and PC, and posterior to the PC. Each of the 12 subcuboids was then either linearly expanded or contracted to match the corresponding subcuboid size defined in the standardized Talairach brain.

Design matrices for the GLM analysis consisted of each participant's stimulation protocol convolved with a hemodynamic response function. Comparisons of BOLD signal amplitude were made between each of the conditions tested (i.e., RF motion vs. open trajectory motion, RF motion vs. static RF patterns, and open trajectory motion vs. static RF patterns). Holm-Bonferroni corrected, two-tailed independent $t$ tests were used to determine whether or not statistically significant differences existed within each region of interest for the tested comparisons. Within each of the three main conditions (i.e., RF motion, open trajectory motion, and static RF patterns), blocks containing different subtypes of the stimulus (for example, RF2 motion and RF3 motion) were pooled for the comparisons of activity related to each main condition.

# Results

## Task proficiency

All participants were able to report the presence of circular trajectories (or analogous straight trajectories or static images of circles) with perfect or near perfect accuracy.

## Summary of general linear model contrast results

The results of the group data region of interest GLM analysis revealed that RF motion trajectory stimuli evoke greater BOLD activity than either open motion trajectories or static images of RF patterns within regions including V1, V2, V3, V3A, and V4 (Table 1). This result was consistent in both hemispheres. Interestingly, in the left but not the right hemisphere static RF patterns also evoked significantly greater BOLD activity than open trajectory visual motion in these same areas. In many of these regions in the right hemisphere there were no significant differences in the amplitude of BOLD activity related to the presentation of open trajectories and static RF patterns.

In contrast, regions MT and STS demonstrated a different pattern of activity. Within these regions, RF motion trajectories and open motion trajectories both evoked greater activity than static RF images except in left MT where there was no significant difference between the RF static and the open trajectory conditions. However, the MT and STS regions of interest showed no significant differences in BOLD activity amplitudes associated with the RF motion and open trajectory motion conditions. Sample group mean time-courses of percentage BOLD signal change are shown in Figure 5.

## Multivoxel pattern analysis (MVPA)

The four classes of RF motion trajectory shapes (i.e., RF2, RF3, RF4, and RF5) could be distinguished with accuracies significantly above the chance level of 25% within visual regions V2 and V3 in both hemispheres (i.e., with a mean classification accuracy of the test data meeting or exceeding the 95th percentile of the distribution obtained via permutation testing; see Figure 6). The number of individual participants in which a significant result was obtained by the classifier in each region of interest is shown in Figure 7. Group mean classification accuracy percentages ($\pm$ standard deviation) were 40.8 $\pm$ 3.6 in left hemisphere V2, 41.4 $\pm$ 4.4 in right V2, 41.2 $\pm$ 2.8 in left V3, and 40.0 $\pm$ 3.5 in right V3.

In addition to examining each of the regions of interest within a single hemisphere, regions were also combined between hemispheres. However, for each region of interest, one-way ANOVAs comparing classification accuracies obtained for left hemisphere, right hemisphere, and regions combined across hemispheres revealed no significant differences as a result of combining regions, V1, $F(2, 27) = 1.08$, $p = 0.35$; V2, $F(2, 27) = 0.481$, $p = 0.62$; V3, $F(2, 27) = 0.54$, $p = 0.59$; V3A, $F(2, 27) = 1.73$, $p = 0.20$; V4, $F(2, 27) = 0.30$, $p = 0.74$; MT, $F(2, 27) = 1.82$, $p = 0.18$; STS, $F(2, 27) = 1.31$, $p = 0.29$.

# Discussion

In the study presented here, we have used fMRI to examine the neural underpinnings of the perception of periodic visual motion. The results of this study demonstrate the following. First, patterns of spatial activity in visual regions V2 and V3 are predictive of the shape of periodic radial frequency (RF) motion trajectories, indicating that these regions are involved

| | Contrast (*t* value, *p*-value) | | |
|---|---|---|---|
| Region of interest | RF motion > RF static | RF motion > open motion | RF static > open motion |
| V1 - LH | 3.13, < 0.005 | 8.68, < 0.005 | 5.55, < 0.005 |
| V1- RH | 4.24, < 0.005 | 7.11, < 0.005 | 2.86, 0.044 |
| V2 - LH dorsal | 3.90, < 0.005 | 9.89, < 0.005 | 5.98, < 0.005 |
| V2 - LH ventral | 3.49, 0.007 | 9.06, < 0.005 | 5.56, < 0.005 |
| V2 - RH dorsal | 5.47, < 0.005 | 6.17, < 0.005 | 0.693, > 0.99 |
| V2 - RH ventral | 2.63, 0.081 | 9.22, < 0.005 | 6.59, < 0.005 |
| V3 - LH dorsal | 4.80, < 0.005 | 10.02, < 0.005 | 5.22, < 0.005 |
| V3 - LH ventral | 3.66, 0.0036 | 10.08, < 0.005 | 6.42, < 0.005 |
| V3 - RH dorsal | 6.67, < 0.005 | 7.97, < 0.005 | 1.29, > 0.99 |
| V3 - RH ventral | 4.06, < 0.005 | 8.97, < 0.005 | 4.90, < 0.005 |
| V3A - LH | 5.39, < 0.005 | 10.51, < 0.005 | 5.12, < 0.005 |
| V3A - RH | 6.51, < 0.005 | 6.85, < 0.005 | 0.328, > 0.99 |
| V4 - LH | 3.87, < 0.005 | 10.69, < 0.005 | 6.82, < 0.005 |
| V4 - RH | 4.78, < 0.005 | 6.77, < 0.005 | 1.99, 0.28 |
| MT - LH | 3.01, 0.036 | 0.792, > 0.99 | −2.23, 0.24 |
| MT - RH | 3.70, 0.0034 | 0.099, 0.92 | *−3.61, < 0.005* |
| STS - LH | 3.66, < 0.005 | −0.591, > 0.99 | *−4.25, < 0.005* |
| STS - RH | 3.49, 0.0065 | −1.85, 0.39 | *−2.67, 0.049* |

Table 1. Results of Holm-Bonferroni corrected *t* test contrasts between BOLD activity evoked by RF motion and comparison stimuli within regions of interest. Adjusted *p*-values are shown. Note that italic values with negative *t* values indicate cases in which open motion trajectories evoked significantly greater activity than static RF images.

in processing this type of visual motion. Second, RF motion trajectories evoke significantly greater activity than do comparable static radial frequency patterns in cortical regions V1, V2, V3, V4, V3A, MT, and STS biomotion regions. Third, RF motion stimuli evoke significantly greater activity than open trajectory visual motion stimuli do in visual regions V1–V4 but not in MT or STS, though the underlying factors leading to this particular result require further examination. In the following sections we discuss the meaning of these findings regarding neurological processing of periodic visual motion.

## Encoding the shape of periodic trajectories in visual regions V2 and V3

Multivoxel pattern analyses (MVPA) demonstrated that within visual regions V2 and V3, RF motion trajectories ranging from two to five cycles can be distinguished based on patterns of spatial activity across voxels. Area V1 was not able to distinguish trajectories indicating that the results in V2 and V3 are not simply a product of local orientation differences in the shapes. Moreover, it is very important to note that the classifier was able to predict the shape of RF trajectories presented within blocks of stimuli that varied in phase and amplitude. The RF trajectories in this study formed recognizable shapes that were oval-like (RF2), triangle-like (RF3), diamond-like (RF4), or star-like (RF5). Thus, it is highly likely that these regions are involved in encoding overall categories of trajectory shape.

The most compelling explanation of this result is that distinct neural populations in V2 and V3 encode the different trajectories. However, several other possibilities must first be considered. Due to the nature of the stimuli, different RF trajectories varied somewhat in path lengths, speeds, and retinotopic extents. Relevant values are shown in Tables 2–4. Considering first path length, all four patterns fall in the range 13.42° to 16.14° and show extensive overlap. Similarly, all fall within a retinotopic range of 1° to 3° from fixation. Finally, the maximum and minimum speeds are extremely similar across patterns. Given that six separate trajectory amplitudes were presented in each block, the vast majority of these exemplars could not have been discriminated based on any of these factors.

Alternatively, participants could have used cognitive strategies that might have influenced the nature of activity seen in the brain such as counting the number of bumps in each trajectory in an attempt to discriminate the RF motion trajectory shapes that they were viewing. However, each block contained only one type of trajectory shape and participants were not asked to overtly identify the shape of individual trajectories within each block but merely to note the presence of circular trajectories with a button press, making this type of strategy unlikely.

Clearly, differences in trajectory curvature are necessary to generate different RF trajectory shapes.

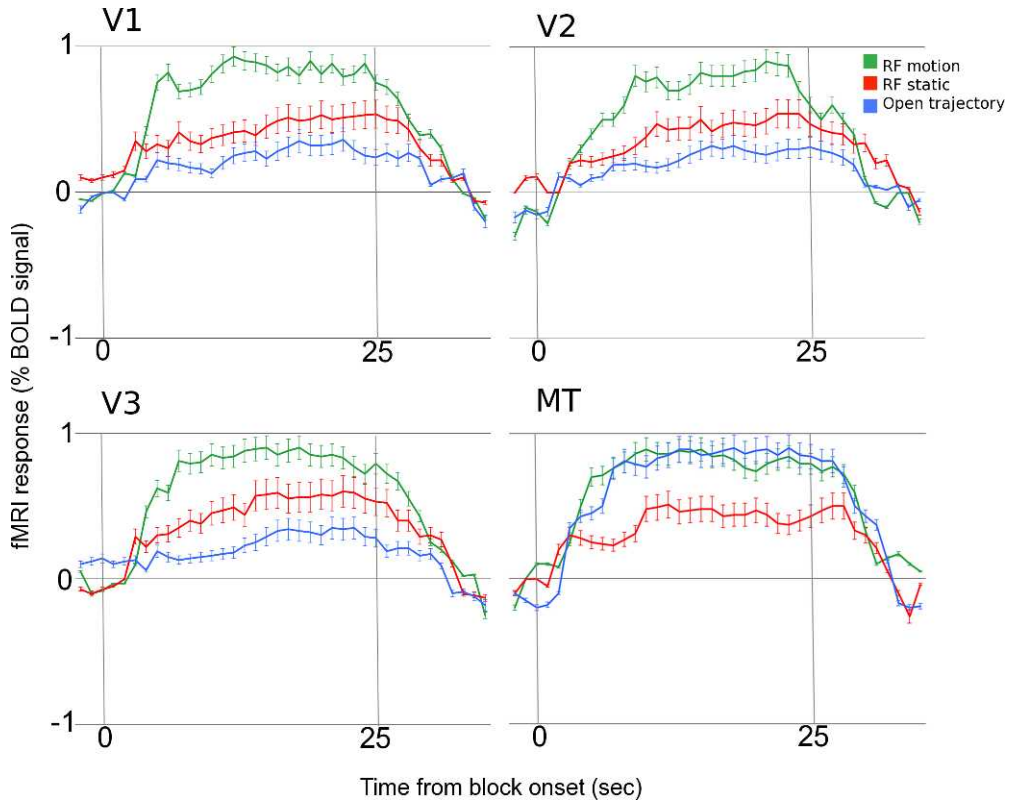


Figure 5. Examples of the time-course of BOLD signal changes time-locked to the onset of stimulus blocks. Time-courses shown are group means collapsed across hemispheres. Error bars represent *SEM*.

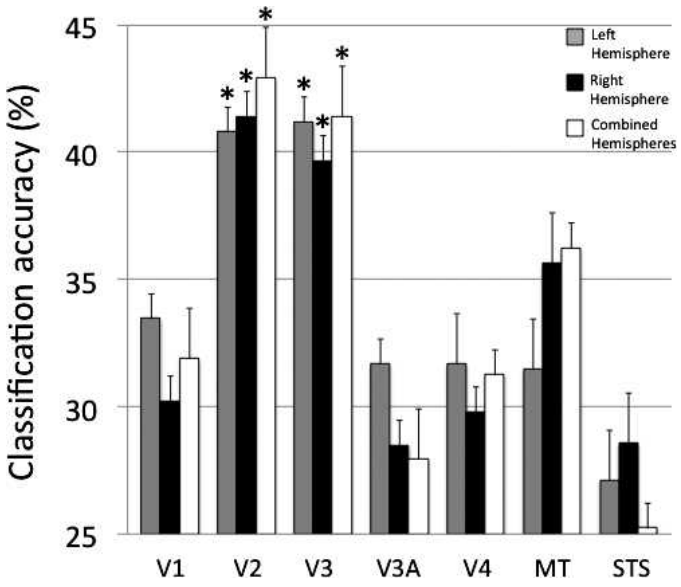


Figure 6. Mean multiclass linear support vector machine classifier accuracy for the discrimination of RF motion trajectories including frequencies ranging from two to five in each region of interest. Significance (*) was defined as a mean classification accuracy of the test data meeting or exceeding the 95th percentile of the distribution obtained with permutation testing.

As there is psychophysical evidence that RF trajectories are processed globally (Or et al., 2011), global representation of trajectories in V2 and V3 is one plausible explanation of our data. However, further study will be needed to disentangle whether V2 and V3 are encoding global properties of the overall shape of trajectories or more local differences in curvature. One attractive hypothesis is that V2 encodes relatively local trajectory curvature, while V3 encodes global RF trajectory shape.

Visual area V2 has been previously demonstrated to be involved in shape representation. For example, a large proportion of V2 cells are selective for complex forms such as angles, arcs, circles, and intersecting lines (i.e., component parts of many different types of shapes; Hegdé & Van Essen, 2000; Ito & Komatsu, 2004). Furthermore, recordings from single cells within V2 demonstrate response modulation and preferences for complex shape stimuli comparable with that observed within visual region V4 (Hegdé & Van Essen, 2007). Similarly, V3 has been shown to be involved in the neural representation of shape. For example, the spatial pattern of activity within V3 demonstrates a functional organization that is related to perceived shape similarity (Op de Beek, Torfs, & Wagemans, 2008). Also in a finding analogous to our result of greater activity for closed motion trajectories compared

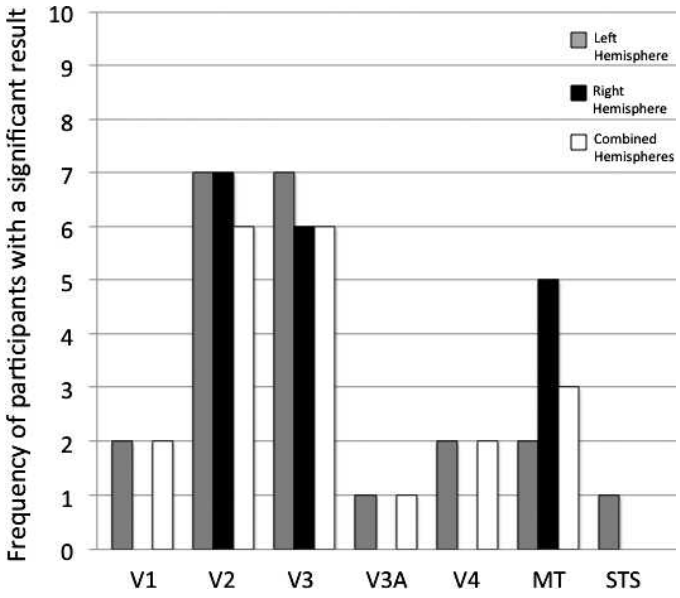


Figure 7. Number of participants in which the multivoxel pattern analysis demonstrated statistically significant discrimination of the four tested frequencies of RF motion trajectories in each region of interest.

with open ones, Dumoulin and Hess (2007) demonstrated that V3 is more strongly activated by static circular Gabor patterns than by static random arrays in which overall curvatures of the constituent elements were similar. In addition, fMRI activity in V2 and V3 (along with many other brain regions) in anesthetized monkeys suggests that these regions are sensitive to three-dimensional shapes defined by motion (Sereno, Trinath, Augath, & Logothetis, 2002). In particular, these regions respond more strongly to rotating computer-generated stimuli made to appear three-dimensional than they do to scrambled versions of these stimuli that lack an impression of depth and shape. Thus, there is evidence in the literature that shapes (both static and defined by motion) are represented within visual areas V2 and V3.

In addition to their involvement in visual shape processing, V2 and V3 are responsive to visual motion in general (Shipp & Zeki, 2002; Vanduffel et al., 2001). Both of these areas exhibit selectivity for the orientation of visual boundaries that are defined solely by motion (Larsson, Heeger, & Landy, 2010; Marcar, Raiguel, Xiao, & Orban, 2000; Reppas, Niyogi, Dale, Sereno, & Tootell, 1997), and motion direction selectivity may be topographically arranged at least within V2 (Lu, Chen, Tanigawa, & Roe, 2010). Furthermore, V2 and V3 are known to share direct reciprocal cortical connections with area MT (Maunsell & van Essen, 1983; Weller, Wall, & Kaas, 1984), a region with a well-known involvement in processing motion. Thus, with a convincing amount of data demonstrating roles in both shape and motion processing, it is not surprising that our data indicate that V2 and V3 are involved in encoding the shape of periodic visual motion trajectories.

| RF | Minimum length (°) | Maximum length (°) |
|---|---|---|
| 2 | 14.44 | 15.40 |
| 3 | 14.41 | 15.84 |
| 4 | 13.42 | 14.99 |
| 5 | 13.87 | 16.14 |

Table 2. Minimum and maximum path lengths of RF motion stimuli used in the experiment.

| RF | Minimum radius (°) | Maximum radius (°) |
|---|---|---|
| 2 | 1 | 3 |
| 3 | 1.27 | 2.73 |
| 4 | 1.53 | 2.47 |
| 5 | 1.53 | 2.47 |

Table 3. Minimum and maximum retinotopic extent of RF motion stimuli used in the experiment.

## No trajectory discrimination in V4, MT, and STS

Multivoxel pattern analyses in V4, MT, and STS did not demonstrate significant differences in patterns of spatial activity associated with different RF motion trajectories. However, before considering what these null findings might suggest, it is important to point out that the absence of a significant ability to distinguish RF motion trajectory shapes with MVPA does not preclude an involvement of these areas in this type of neurological processing. For example, it is possible that the organization of neural responses within certain regions is not amenable to detection by fMRI multivoxel analysis (for example, distributed rather than topographical neurological responses).

The MVPA classifier was unable to discriminate between RF motion trajectories within V4. Thus, our data do not provide evidence in favor of a view that V4 is involved in encoding the specific shapes of periodic motion trajectories. This result was surprising to us since neural activity within V4 is known to be associated with shape perception (see Pasupathy,

| RF | Minimum speed (°/s) | Maximum speed (°/s) | Mean speed |
|---|---|---|---|
| 2 | 3.14 | 9.60 | 7.70 |
| 3 | 3.98 | 9.60 | 7.92 |
| 4 | 4.82 | 8.75 | 7.50 |
| 5 | 4.82 | 9.74 | 8.07 |

Table 4. Minimum and maximum speed of dot motion in RF motion stimuli used in the experiment.

2006) and cells in this region are sensitive to visual motion (Cheng, Hasegawa, Saleem, & Tanaka, 1994; Vinberg & Grill-Spector, 2008), making V4 a good potential candidate for an involvement in the processing of RF motion trajectory shapes. Furthermore, Gallant, Connor, Rakshit, Lewis, and Van Essen (1996) demonstrated that V4 cells selective for specific categories of static shapes such as hyperbolic, radial, and concentric gratings are somewhat segregated anatomically. Our RF trajectories are similar in nature to their concentric stimuli. However, it is not known whether or not the neural responses within these segregated clusters are also topographically organized or haphazardly distributed. If the latter, it would not be surprising if RF shapes or trajectories, which would all be expected to activate neurons within the concentric clusters, failed to produce significant multivoxel analysis results. Thus, further examination of how neuronal activity is organized in V4 for both static shapes and motion trajectories is required before definite conclusions can be drawn regarding this region's specific roles in the perception of periodic motion.

A lack of RF motion trajectory discrimination in area MT was also somewhat surprising to us given this region's well-known role in visual motion perception. MT possesses a columnar organization of neurons that selectively respond to specific directions of motion (Dubner & Zeki, 1971; Zimmermann et al., 2011). However, given that MT does not seem to be sensitive to motion-defined boundaries (Larsson et al., 2010, Marcar, Xiao, Raiguel, Maes, & Orban, 1995; Reppas et al., 1997), it is possible that this region is more suited for the processing of overall global directions of visual motion, such as optic flow, rather than categorizing the shapes of motion trajectories. On the other hand, Figure 7 reveals that the proportion of participants with a significant decoding result in region MT appears somewhat higher than one might predict it would from noise alone. This suggests that perhaps MT does have a role in processing the shape of periodic visual motion trajectories that we simply could not consistently detect with the methods used in the current study.

Finally, our multivoxel analyses did not reveal significant differences in patterns of activity for different RF motion shapes within biological motion related regions of the STS. Periodic motion forms an integral component of many types of biological movements (for example, Johansson, 1973; Tsai et al., 1994; Xiong & Quek, 2006). Our results therefore suggest that superior temporal sulcus biological motion regions are more concerned with processing global aspects of biological motion rather than individual components comprising body movement. Components of biological movement including both closed and open trajectory information may be combined at this level. It is quite possible that information related to the processing of periodic movements in regions V2 and/or V3 could be passed on to STS biomotion-related regions and incorporated into a global representation of movement of the body as a whole. In fact, V3 activity has been observed during biological motion perception (Howard et al., 1996) and has been suggested to play an important role in the perception of biological motion (Servos, Osu, Santi, & Kawato, 2002) making our finding of the encoding of periodic visual motion trajectory shapes in V3 especially intriguing.

## Comparisons of periodic trajectories, static shapes, and open path trajectories

Levels of BOLD fMRI activity within regions of interest in the visual system were compared for periodic radial frequency visual motion trajectories, static images of RF shapes, and open sinusoidal movement trajectories. Activity associated with RF motion and static RF shapes was contrasted within regions of interest V1, V2, V3, V3A, V4, MT, and STS. BOLD signal amplitude associated with RF motion was significantly and consistently higher in all regions (Table 1). Motion and static RF stimuli were carefully equated for presentation duration, number of stimuli presented, phase, amplitude, retinotopic extent, and spatial frequency bandwidth meaning that the only characteristic of the stimuli that differed was whether the shapes were presented all at once in a still form or over the duration of the trial as a motion trajectory. The underlying factors contributing to this difference merit further investigation. Adaptation in the case of the 3.3 s static patterns or differential contribution of magnocellular and parvocellular pathways are two factors that could be relevant.

Comparisons of BOLD activity associated with RF motion and open trajectory motion also revealed greater activity for RF motion but only within regions V1, V2, V3, V3A, and V4. In MT and STS, both regions known to be highly involved in motion analysis, the two forms of motion produced equivalent levels of BOLD activity (see Table 1). While it would be appealing to conclude that neural processing of open and closed visual motion is accomplished differently in the early topographic areas, there are other factors that may have contributed to this difference.

Selecting an appropriate open-trajectory comparison was difficult as it was not possible to equate all relevant parameters in one stimulus. The open trajectories used were selected to match the RF trajectories in three respects: the time to trace the trajectory was equal (3.3 s/stimulus), both entailed two or three cycles of sinusoidal deviation—either from a straight line or from a perfect circle, and both entailed a single

continuous non-broken trajectory. However, achieving these conditions meant that the total contour length for an individual trajectory was shorter for the open than the closed trajectories and that the speed of dot motion was slower for the open than for the closed trajectory. Either of these factors could be reflected in the difference seen in early visual areas. An additional factor that could be only partially equated was retinal eccentricity. The radius of the circular trajectory and the distance of the straight line trajectory from the fixation point at the vertical meridian were 2° in each case; thus around the vertical meridian the various trajectory paths covered roughly the same range of eccentricities in both the upper and lower fields. However, because we used only horizontal open trajectories, the moving dots never crossed the horizontal meridian. Furthermore, any given open trajectory exemplar spent twice as long in two visual quadrants (upper left and right, or lower left and right) than the closed trajectory, which moved through all four quadrants on each presentation. However, over the set of trajectories in one block in our block design, the average stimulation time in each quadrant was equated. One approach to disentangling these factors would be to introduce multiple open trajectories in different orientations and field regions, either simultaneously or successively. Alternatively, randomized sectors of the closed contour in nonsequential order could be compared to the RF trajectories used here. However, these controls introduce their own confounds and the number of necessary permutations was beyond the scope of the present study.

The observation of a stronger BOLD response to closed than to open trajectories in V4 but not in MT and STS, does lend some credence to the view that the V4 difference and those seen in the earlier visual areas reflect the extraction of global shape properties of the trajectories rather than low level motion differences, since one would have expected that MT in particular would be sensitive to factors such as speed and total trajectory length. Another possible approach would be to examine the effect of contrast variation on the two forms of motion. The contrast dependence of detection thresholds for static RF patterns versus static open sinusoidal trajectories, as assessed psychophysically, has been reported to differ (Wilkinson et al., 1998).

## Conclusions

The data presented here demonstrate that the pattern of spatial activity in visual regions V2 and V3 is predictive of the shape of periodic movement trajectories, thus indicating that these regions are involved in encoding this type of information. Further, periodic visual motion evokes greater BOLD activity than comparable static shapes in regions V1–V4, MT, and biological motion related regions of STS. Finally, the results of the study also suggest that the neural processing of closed-circuit periodic visual motion may differ from that associated with processing of open trajectory motion. Overall, the results of the study provide an interesting first look at the neural correlates of the perception of periodic visual motion and they indicate that periodic motion perception should form an important new domain for visual motion studies.

## Acknowledgments

The authors would like to thank Randolph Blake for providing the point light animations used to localize brain regions involved in biological motion processing. This work was supported by NSERC Discovery Grants #227224 to HRW and #007551 to FW.

Commercial relationships: none.
Corresponding author: Diana J. Gorbet.
Email: dgorbet@alumni.yorku.ca.
Address: Centre for Vision Research, York University, Toronto, ON, Canada.

## References

Barclay, C. D., Cutting, J. E., & Kozlowski, L. T. (1978). Temporal and spatial factors in gait perception that influence gender recognition. *Perception & Psychophysics, 23*, 145–152.

Chang, D. H. F., & Troje, N. F. (2009). Acceleration carries the local inversion effect in biological motion perception. *Journal of Vision, 9*(1):19, 1–17, http://www.journalofvision.org/content/9/1/19, doi:10.1167/9.1.19. [PubMed] [Article]

Cheng, K., Hasegawa, T., Saleem, K. S., & Tanaka, K. (1994). Comparison of neuronal selectivity for stimulus speed, length, and contrast in the prestriate visual cortical areas V4 and MT of the macaque monkey. *Journal of Neurophysiology, 71,* 2269–2280.

Dittrich, W. H., Troscianko, T., Lea, S. E. G., & Morgan, D. (1996). Perception of emotion from dynamic point-light displays represented in dance. *Perception, 25,* 727–738.

Dubner, R., & Zeki, S. M. (1971). Response properties and receptive fields of cells in an automatically defined region of the superior temporal sulcus in the monkey. *Brain Research, 35,* 528–532.

Dumoulin, S. O., & Hess, R. F. (2007). Cortical specialization for concentric shape processing. *Vision Research, 47,* 1608–1613.

Engel, S. A., Glover, G. H., & Wandell, B. A. (1997). Retinotopic organization in human visual cortex and the spatial precision of functional MRI. *Cerebral Cortex, 7,* 181–192.

Gallant, J. L., Connor, C. E., Rakshit, S., Lewis, J. W., & Van Essen, D. C. (1996). Neural responses to polar, hyperbolic, and Cartesian gratings in area V4 of the macaque monkey. *Journal of Neurophysiology, 76,* 2718–2739.

Grossman, E., Donnelly, M., Price, R., Pickens, D., Morgan, V., Neighbor, G. et al. (2000). Brain areas involved in perception of biological motion. *Journal of Cognitive Neuroscience, 12*, 711–720.

Grossman, E. D., & Blake, R. (2001). Brain activity evoked by inverted and imagined biological motion. *Vision Research, 41,* 1475–1482.

Hegdé, J., & Van Essen, D. C. (2000). Selectivity for complex shapes in primate visual area V2. *Journal of Neuroscience, 20*, RC61–RC66.

Hegdé, J., & Van Essen, D. C. (2007). A comparative study of shape representation in macaque visual areas V2 and V4. *Cerebral Cortex, 17,* 1100–1116.

Hirai, M., Saunders, D. R., & Troje, N. F. (2011). Allocation of attention to biological motion: Local motion dominates global shape. *Journal of Vision, 11*(3):4, 1–11, http://www.journalofvision.org/content/11/3/4, doi:10.1167/11.3.4. [PubMed] [Article]

Howard, R. J., Brammer, M., Wright, I., Woodruff, P. W., Bullmore, E. T., & Zeki, S. (1996). A direct demonstration of functional specialization within motion-related visual and auditory cortex of the human brain. *Current Biology, 6,* 1015–1019.

Ito, M., & Komatsu, H. (2004). Representation of angles embedded within contour stimuli in area V2 of macaque monkeys. *The Journal of Neuroscience, 24,* 3313–3324.

Johansson, G. (1973). Visual-perception of biological motion and a model for its analysis. *Perception & Psychophysics, 14*, 201–211.

Johansson, G. (1976). Spatio-temporal differentiation and integration in visual motion perception. An experimental and theoretical analysis of calculus-like functions in visual data processing. *Psychological Research, 38,* 379–393.

Ladewig, S. H. (2011). Putting the cyclic gesture on a cognitive basis. *CogniTextes, 6,* 1–25.

Larsson, J., Heeger, D. J., & Landy, M. S. (2010). Orientation selectivity of motion- boundary responses in human visual cortex. *Journal of Neurophysiology, 104,* 2940–2950.

Lu, H. D., Chen, G., Tanigawa, H., & Roe, A. W. (2010). A motion direction map in macaque V2. *Neuron, 68,* 1002–1013.

Marcar, V. L., Raiguel, S. E., Xiao, D., & Orban, G. A. (2000). Processing of kinetically defined boundaries in areas V1 and V2 of the macaque monkey. *Journal of Neurophysiology, 84,* 2786–2798.

Marcar, V. L., Xiao, D.-K., Raiguel, S. E., Maes, H., & Orban, G. A. (1995). Processing of kinetically defined boundaries in the cortical motion area MT of the macaque monkey. *Journal of Neurophysiology, 74,* 1258–1270.

Mather, G., & Murdoch, L. (1994). Gender discrimination in biological motion displays based on dynamic cues. *Proceedings of the Royal Society B: Biological Sciences, 258,* 273–279.

Maunsell, J. H. R., & van Essen, D. C. (1983). The connections of the middle temporal visual area (MT) and their relationship to a cortical hierarchy in the macaque monkey. *The Journal of Neuroscience, 3,* 2563–2586.

Misaki, M., Kim, Y., Bandettini, P. A., & Kriegeskorte, N. (2010). Comparison of multivariate classifiers and response normalizations for pattern-information fMRI. *NeuroImage, 53,* 103–118.

Nichols, T. E., & Holmes, A. P. (2001). Nonparametric permutation tests for functional neuroimaging: A primer with examples. *Human Brain Mapping, 15,* 1–25.

Op de Beek, H. P., Torfs, K., & Wagemans, J. (2008). Perceived shape similarity among unfamiliar objects and the organization of the human object vision pathway. *The Journal of Neuroscience, 28,* 10111–10123.

Or, C. C.-F., Thabet, M., Wilkinson, F., & Wilson, H. R. (2011). Discrimination and identification of periodic motion trajectories. *Journal of Vision, 11*(8):7, 1–11, http://www.journalofvision.org/content/11/8/7, doi:10.1167/11.8.7. [PubMed] [Article]

Pasupathy, A. (2006). Neural basis of shape representation in the primate brain. *Progress in Brain Research*, *154*, 293–313.

Peelen, M. V., & Wiggett, A. J. (2006). Patterns of fMRI activity dissociate overlapping functional brain areas that respond to biological motion. *Neuron, 49*, 815–822.

Rainville, S. J. M., & Wilson, H. R. (2004). The influence of motion-defined form on the perception

of spatially-defined form. *Vision Research, 44,* 1065–1077.

Reppas, J. B., Niyogi, S., Dale, A. M., Sereno, M. I., & Tootell, R. B. H. (1997). Representation of motion boundaries in retinotopic human visual cortical areas. *Nature, 388,* 175–179.

Sereno, M. I., Dale, A. M., Reppas, J. B., Kwong, K. K., Belliveau, J. W., Brady, T. J. et al. (1995). Borders of multiple visual areas in humans revealed by functional magnetic resonance imaging. *Science, 268,* 889–893.

Sereno, M. E., Trinath, T., Augath, M., & Logothetis, N. K. (2002). Three-dimensional shape representation in monkey cortex. *Neuron*, *33*, 635–652.

Servos, P., Osu, R., Santi, A., & Kawato, M. (2002). The neural substrates of biological motion perception: An fMRI study. *Cerebral Cortex, 12,* 772–782.

Shipp, S., & Zeki, S. (2002). The functional organization of area V2, I: Specialization across stripes and layers. *Visual Neuroscience, 19,* 187–210.

Slotnick, S. D., & Yantis, S. (2003). Efficient acquisition of human retinotopic maps. *Human Brain Mapping, 18,* 22–29.

Todd, J. T. (1982). Visual information about rigid and non-rigid motion: A geometric analysis. *Journal of Experimental Psychology: Human Perception and Performance, 8,* 238–252.

Tootell, R. B. H., Reppas, J. B., Kwong, K. K., Malach, R., Born, R. T., Brady, T. J. et al. (1995). Functional analysis of human MT and related visual cortical areas using magnetic resonance imaging. *The Journal of Neuroscience, 15,* 3215–3230.

Troje, N. F. (2002). Decomposing biological motion: A framework for analysis and synthesis of human gait patterns. *Journal of Vision*, *2*(5):2, 371–387, http://www.journalofvision.org/content/2/5/2, doi:10.1167/2.5.2. [PubMed] [Article]

Troje, N. F., & Westhoff, C. (2006). The inversion effect in biological motion perception: Evidence for a "life detector"? *Current Biology, 16*, 821–824.

Tsai, P.-S., Shah, M., Keiter, K., & Kasparis, T. (1994). Cyclic motion detection for motion based recognition. *Pattern Recognition, 27,* 1591–1603.

Vanduffel, W., Fize, D., Mandeville, J. B., Nelissen, K., Van Hecke, P., Rosen, B. R. et al. (2001). Visual motion processing investigated using contrast agent-enhanced fMRI in awake behaving monkeys. *Neuron, 32,* 565–577.

Vinberg, J., & Grill-Spector, K. (2008). Representation of shapes, edges, and surfaces across multiple cues in the human visual cortex. *Journal of Neurophysiology, 99,* 1380–1393.

Watson, J. D. G., Myers, R., Frackowiak, R. S. J., Hajnal., J. V., Woods, R. P., Mazziotta, J. C. et al. (1993). Area V5 of the human brain: Evidence from a combined study using positron emission tomography and magnetic resonance imaging. *Cerebral Cortex, 3,* 79–94.

Weller, R. E., Wall, J. T., & Kaas, J. H. (1984). Cortical connections of the middle temporal visual area (MT) and the superior temporal cortex in owl monkeys. *The Journal of Comparative Neurology, 228,* 81–104.

Wilkinson, F., Wilson, H. R., & Haback, C. (1998). Detection and recognition of radial frequency patterns. *Vision Research, 38*, 3555–3568.

Xiong, Y., & Quek, F. (2006). Hand motion gesture frequency properties and multimodal discourse analysis. *International Journal of Computer Vision, 69,* 353–371.

Zeki, S., Watson, J. D. G., Lueck, C. J., Friston, K. J., Kennard, C., & Frackowiak, R. S. J. (1991). A direct demonstration of functional specialization in human visual cortex. *The Journal of Neuroscience, 11,* 641–649.

Zimmermann, J., Goebel, R., De Martino, F., van de Moortele, P.-F., Feinberg, D., Adriany, G. et al. (2011). Mapping the organization of axis of motion selective features in human area MT using high-field fMRI. *PLoS ONE, 6,* e28716.